International Journal of Innovative
Computing, Information and Control
Volume **19**, Number **2**, April **2023**

ICIC International ©2023 ISSN 1349-4198
pp. **487–502**

PRESCRIBED PERFORMANCE BASED MODEL-FREE FRACTIONAL-ORDER SLIDING MODE CONTROL FOR PERMANENT MAGNET LINEAR SYNCHRONOUS MOTOR

Jing Hu, Dezhi Xu*, Weiming Zhang and Weilin Yang

School of Internet of Things Engineering
Jiangnan University
No. 1800, Lihu Avenue, Wuxi 214122, P. R. China
{ 6201925009; wmzhang }@stu.jiangnan.edu.cn; wlyang@jiangnan.edu.cn
*Corresponding author: xudezhi@jiangnan.edu.cn

Received July 2022; revised November 2022

Abstract. *In this paper, a prescribed performance based model-free fractional-order sliding mode control is proposed to improve the speed tracking capability and robustness of permanent magnet linear synchronous motor (PMLSM). Firstly, a dynamic model of PMLSM is established. Then a prescribed performance control is proposed to ensure that the tracking error is within the boundary of the prescribed performance function. On this basis, the ultra-local model of the speed loop is given according to the input and output of the PMLSM system. The extended state observer is established to estimate the internal and external total disturbance, and the speed loop controller is fed forward compensation. Finally, the feedback controller is designed as fractional-order sliding mode control to converge the system state to the origin point in a finite time and improve the system's robustness effectively. Simulation results and experiments in dSPACE demonstrate the advantages and effectiveness of the proposed controller.*

Keywords: Permanent magnet linear synchronous motor, Prescribed performance, Model-free control, Fractional-order sliding mode control, Extended state observer

1. **Introduction.** Compared with the traditional rotary motor, the linear motor eliminates the complex transmission structure, which belongs to a direct drive system. PMLSM has the advantages of high thrust density, sensitive response speed, high precision, simple structure, and small mechanical loss. Currently, PMLSM has been widely used in robotics, urban rail transit, high-grade CNC machine tools, and other fields [1-3]. However, when PMLSM is running, it will be affected by groove effect, end effect, force of friction, load disturbance, and parameter variations, resulting in speed precision and anti-interference of PMLSM are poor [4]. To reduce the adverse effects caused by these problems, appropriate control strategies must be adopted to achieve high precision control of PMLSM [5].

With the continuous research of scholars, many advanced control methods have been applied to PMLSM such as model predictive control (MPC) [6,7], fuzzy control (FC) [8], and neural network control (NNC) [9]. However, the above methods not only require a lot of calculation, but also have a large steady-state error, which may cause the system to lose stability. Sliding mode control (SMC) has been widely used in PMLSM servo systems due to its strong robustness, insensitivity to parameter variations, and fast response speed [10,11]. Since SMC belongs to discontinuous control, it is inevitable that the controlled system chatters. When the sliding surface is switched at high speed, frequent chattering will occur, which will lead to system performance degradation and even

DOI: 10.24507/ijicic.19.02.487

system crash. Therefore, how to reduce chattering is always the focus of the SMC. Usually, the advanced reaching law, dynamic nonlinear sliding mode surface, and disturbance observer compensation are designed to reduce chattering. In [12], an angle-based saturation function was used to effectively eliminate the chattering of complementary SMC and improved the position tracking precision of PMLSM. However, the dynamic response of this control strategy was not strong. In [13], an adaptive neural network nonsingular fast terminal SMC method was proposed. The proposed control strategy could avoid the singularity problem and make PMLSM have the advantages of fast convergence of state variables, strong robustness, and good response performance. However, the design process was complicated and the parameters are complicated to adjust. A high-order fast nonsingular terminal SMC strategy based on double disturbance observers was presented in [14]. This strategy could effectively improve the position tracking precision and robustness of PMLSM to multiple disturbances. However, it failed to achieve the prescribed overshoot and steady-state error.

Since the SMC is essentially a control algorithm based on the model, the precision of the mathematical model of the controlled object affects the performance of the SMC. In order to reduce the dependence on mathematical models, scholars put forward model-free control (MFC). MFC was born in the 1970s and has been developing till now. Scholars Fliess and Join extended the MFC and proposed an ultra-local model (ULM) [15]. Its basic idea is to establish the ULM by using the input and output values of the system, and then the controller is designed on the basis of the ULM. Since SMC has strong robustness and anti-interference, it is usually combined with MFC to obtain better control performance. A control strategy combining MFC and integral SMC was proposed in [16]. Double disturbance feedforward compensation is adopted to improve the convergence speed and anti-interference ability of the motor. Currently, there are few studies on the control strategies combining MFC and SMC for PMLSM, so it is necessary to carry out relevant studies. In addition, the estimation precision of unknown parts in MFC will significantly impact the control system. For this problem, parameter identification and estimation technology were introduced in [17], which realized the fast estimation of disturbance. However, it is susceptible to the influence of control signal noise. In [18], a model-free predictive current controller was designed and the extended state observer (ESO) was given to observe the total internal and external disturbances of the motor. The control strategy made the motor have good performance in current harmonics, tracking error, and dynamic overshoot.

Fractional-order calculus was invented by Leibniz and Newton at the end of the 17th century [19]. Previously, it was considered as a purely theoretical discipline with few field applications. However, in the past three decades, its application in control systems has attracted more and more attention [20-22]. In control practice, the sliding mode surface of SMC is usually designed as an integer order. By using the memory and genetic properties of fractional operators to construct integral or differential order sliding mode surfaces of state variables, higher control precision, and extra freedom can be obtained. In [23], a fractional-order sliding mode control (FOSMC) combining adaptive and fuzzy control strategy was proposed. The fractional-order integral term was introduced into SMC, which could effectively enhance the tracking precision of the PMLSM. A cross-coupled second-order discrete-time FOSMC strategy was proposed in [24]. The fractional-order sliding mode surface could reduce the chattering phenomenon and improve the dynamic response performance. This control strategy effectively realized the precise synchronous control of PMLSM.

In order to reduce the tracking error and improve system stability, prescribed performance control (PPC) has been proposed in [25,26]. The core idea of PPC is to transform

the errors of the old system into the errors of the new system by using the prescribed performance function (PPF). This converted error is used to replace the original error in the controller. When the transformation error is bounded, the original error can be guaranteed to be within the prescribed boundary. This algorithm has been widely used in nonlinear systems such as vehicle systems [27], robot systems [28], and ship systems [29].

Inspired by the analysis of previous research results, this paper takes PMLSM as the research object and designs a prescribed performance based model-free fractional-order sliding mode controller. When PMLSM encounters lumped disturbance, motor parameter variations, and other adverse effects, the control strategy achieves accurate speed tracking and robust control, accelerates the rapid convergence of the system state to the equilibrium point, and restraps chattering phenomenon to a certain extent. The superiority and effectiveness of the proposed control strategy are proved by simulation results in MATLAB and experimental results in dSPACE. Compared with the existing research results, the main contributions of this paper are summarized as follows:

1) PPC is adopted to ensure the speed tracking error of PMLSM within the specified range and reduce the speed overshoot;
2) The ULM is established according to the input and output of the speed loop and ESO is used to observe the internal and external total disturbance of the system and carry out feedforward compensation, improving the anti-interference performance of PMLSM effectively;
3) The feedback controller is designed as FOSMC, which guarantees finite time stability and robustness of the system.

The organization of this paper is as follows. The mathematical model of PMLSM and the definition of fractional-order calculus are given in Section 2. The derivation process and stability analysis of the proposed method are presented in Section 3. Section 4 analyzes the simulation results and experimental results, proving that the proposed method has favorable performance in the control of PMLSM. Finally, Section 5 comes to the conclusion.

2. **Mathematical Description and Preliminaries.**

In this section, the mathematical model of PMLSM is established and the basic definition of fractional-order calculus is given.

2.1. **Problem formulation for PMLSM.**

The primary component (winding) of the linear motor can be regarded as cutting and flattening the stator part of the permanent magnet synchronous motor (PMSM). Similarly, the secondary component (permanent magnet) can be regarded as the rotor part of PMSM. When the primary component of PMLSM is connected to the AC power supply, a horizontal moving magnetic field will be generated, which is also known as a traveling wave magnetic field. The traveling wave magnetic field and the permanent magnet will interact to produce electromagnetic thrust and drive the primary component to move in a straight line. Figure 1 illustrates the linear motor structures schematically. PMLSM is a strongly coupled and multivariable nonlinear system. For the convenience of analysis, the following assumptions are made: there is no armature reaction in the air gap; the excitation magnetic field, and the armature reaction magnetic field are sinusoidal distributions; do not consider the magnetic saturation effect, eddy current, and hysteresis loss in the PMLSM. Therefore, the voltage equation of surface-mounted PMLSM in the d-q coordinate system can be formulated as follows

$$\begin{cases} u_d = R_s i_d + L_d \dfrac{di_d}{dt} - \omega_e L_q i_q \\ u_q = R_s i_q + L_q \dfrac{di_q}{dt} + \omega_e \left(L_d i_d + \varphi_f\right) \end{cases} \tag{1}$$

where u_d, u_q are stator voltages in d-q frame; i_d, i_q are stator current in d-q frame; R_s is stator resistance; L_d, L_q are stator inductance in d-q frame; for a surface-mounted PMLSM, the stator inductance satisfies $L_d = L_q$; φ_f is the permanent magnet flux linkage; ω_e is the electrical angular velocity. ω_e can be expressed as

$$\omega_e = \frac{\pi v}{\tau} \tag{2}$$

where v is the speed of the mover, and τ is pole pitch.

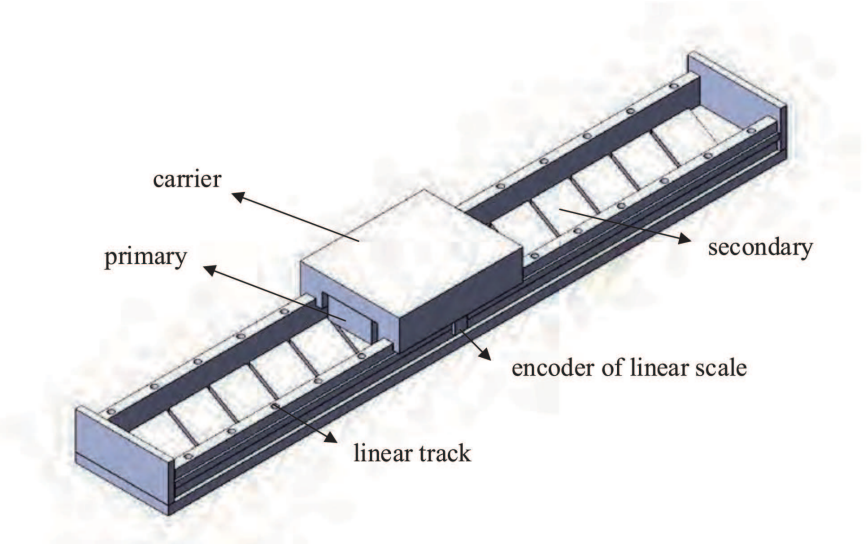

FIGURE 1. Structural diagram of PMLSM

The magnetic field-oriented control (FOC) method with $i_d^* = 0$ is adopted in this paper. Since $L_d = L_q$, electromagnetic thrust F_e can be simplified as

$$F_e = \frac{3\pi n_p \varphi_f}{2\tau} i_q \tag{3}$$

where n_p is pole pairs.

The mechanical motion equation of PMLSM can be expressed as

$$\begin{cases} F_e = M\dot{v} + Bv + d \\ d = F_L + F_f + F_r \end{cases} \tag{4}$$

where M is the mover mass, B is the viscous friction coefficient, d is the nonlinear disturbance, F_L is the load disturbance, F_f is the friction force, and F_r is the thrust ripple.

Finally, the simplified motion equation of PMLSM can be expressed as

$$\begin{cases} \dfrac{dv}{dt} = \dfrac{3\pi n_p \varphi_f}{2\tau M} i_q - \dfrac{B}{M} v - \dfrac{d}{M} \\ \dfrac{di_d}{dt} = \dfrac{1}{L_d} u_d + \dfrac{\pi}{\tau} v i_q - \dfrac{R_s}{L_d} i_d \\ \dfrac{di_q}{dt} = \dfrac{1}{L_q} u_q - \dfrac{\pi}{\tau} v i_d - \dfrac{R_s}{L_q} i_q - \dfrac{\pi \varphi_f}{L_q \tau} v \end{cases} \tag{5}$$

2.2. **Fractional-order calculus.** The fractional-order calculus of functions can provide more information than integer calculus. The fractional-order calculus has been further developed based on the integer calculus. Various definitions of fractional-order calculus emerged during its development. Among them, the Riemann-Liouville definition is one of the most widely used in practical engineering, which is adopted in this paper.

Definition 2.1. *Riemann-Liouville fractional calculus is defined as follows [30]*

$$\begin{cases} {}_{t_0}^{RL}D_t^{\kappa}g(t) = \dfrac{1}{\Gamma(n-\kappa)}\dfrac{d^n}{dt^n}\displaystyle\int_{t_0}^{t}\frac{g(\varpi)}{(t-\varpi)^{1+\kappa-n}}d\varpi \\ {}_{t_0}^{RL}D_t^{-\kappa}g(t) = \dfrac{1}{\Gamma(\kappa)}\displaystyle\int_{t_0}^{t}\frac{g(\varpi)}{(t-\varpi)^{1-\kappa}}d\varpi \end{cases} \tag{6}$$

where t_0 and t are the limits of the operation, κ is the order of operation, $n-1<\kappa\leqslant n$, n is the integer, and $\Gamma(x)=\int_0^{\infty}t^{x-1}e^{-t}dt$ is the Gamma function.

For convenience, the following sections use D^{κ} instead of ${}_{t_0}^{RL}D_t^{\kappa}$.

Remark 2.1. *If the order of operation $\kappa=0$, then $D^{\kappa}g(t)=g(t)$.*

Remark 2.2. *If the order of operation $\kappa>0$, D^{κ} stands for fractional-order differential operator and $D^{-\kappa}$ stands for fractional-order integral operator.*

3. Controller Design.

3.1. **Prescribed performance function.** To ensure that the speed tracking error is always within the prescribed performance range, PPC is introduced. The speed error of PMLSM is defined as follows

$$e = v - v^* \tag{7}$$

where v is the actual speed, and v^* is the given speed.

The error e satisfies the following inequality

$$-\underline{\eta}\mu(t) < e(t) < \bar{\eta}\mu(t) \tag{8}$$

where $\underline{\eta}$, $\bar{\eta}$ are positive constants. PPF can be selected as follows

$$\mu(t) = (\mu_0 - \mu_\infty)e^{-lt} + \mu_\infty \tag{9}$$

where l, μ_0, μ_∞ are positive constants, $\mu_0>\mu_\infty>0$, μ_0 is the initial values of the PPF, μ_∞ is the final boundary of error, and l is the convergence rate of the boundary.

A smooth and strictly increasing function can be chosen as follows

$$S(\varepsilon) = \frac{\bar{\eta}e^{\varepsilon} - \underline{\eta}\ e^{-\varepsilon}}{e^{\varepsilon}+e^{-\varepsilon}} \tag{10}$$

where ε is the transformed error. Therefore, (8) can be rewritten as

$$e(t) = \mu(t)S(\varepsilon) \tag{11}$$

Then the transformed error can be expressed as

$$\varepsilon(t) = \frac{1}{2}\ln\frac{\underline{\eta}+e(t)/\mu(t)}{\bar{\eta}-e(t)/\mu(t)} \tag{12}$$

By introducing a smooth reversible function $S(\varepsilon)$, the inequality constraint in (8) can be transformed into an unconstrained form as shown in (11). Meanwhile, the feedback control law is constructed to ensure that the transformation error ε is stable and the prescribed performance index is satisfied.

3.2. **Ultra-local model.** For a multivariable single input and single output (SISO) system that is first-order nonlinear and complex, it can be replaced by ULM, which is defined as [15]

$$\dot{y} = \alpha u + F \tag{13}$$

where y and u represent the output and input of the system, α is the gain of the input, and F is the sum of internal disturbances and external disturbances of the system.

According to the ULM, the MFC of the system can be expressed as

$$u = \frac{-\hat{F} + \dot{y}^* + \vartheta}{\alpha} \tag{14}$$

where $\hat{F}$ is the estimated value of F, y^* is the expected output of the system, and ϑ can be PI, SMC or other controllers.

According to (5), v and i_q can be taken as system output and system input to establish ULM structure, which can be defined as

$$\frac{dv}{dt} = \alpha_v i_q + F_v \tag{15}$$

where $\alpha_v = 3\pi n_p \varphi_f/(2\tau M)$, $F_v = -(Bv + d)/M$. The speed loop ULM can be expressed as

$$i_q = \frac{-\hat{F}_v + \dot{v}^* + u_s}{\alpha_v} \tag{16}$$

where $\hat{F}_v$ is estimate of the sum of internal and external disturbances, and u_s is the designed feedback controller.

3.3. **ESO parameter design.** In order to observe the unknown disturbances in the ULM, ESO is established. The ESO expands the nth-order system to the $(n+1)$th-order system, which can observe the sum of the internal state variables and internal and external disturbances of the system. According to (15), v and F_v are selected as variables and system unmodeled variables. Second-order ESO can be designed as

$$\begin{cases} e_r = z_1 - v \\ \dot{z}_1 = z_2 + \alpha_v i_q - \beta_1 e_r \\ \dot{z}_2 = -\beta_2 e_r \end{cases} \tag{17}$$

where z_1 is the observed value of v, $z_1 = \hat{v}$; z_2 is the observed value of the unmodeled part of the system, $z_2 = \hat{F}_v$; β_1 and β_2 are the error feedback gain coefficient of ESO. According to (17), we obtain the characteristic equation of ESO

$$s^2 + \beta_1 s + \beta_2 = 0 \tag{18}$$

In order to make ESO state stable, the characteristic root of the characteristic equation is $-\omega_n$. The gain coefficient of ESO is

$$\begin{cases} \beta_1 = 2\omega_n \\ \beta_2 = \omega_n^2 \end{cases} \tag{19}$$

ω_n represents bandwidth, which determines the dynamic characteristics and stability of ESO. ω_n should be large enough to ensure that the dynamics of the ESO are fast enough to track changes in the total disturbance. In addition, the larger the bandwidth, the more sensitive ESO is to sampling noise. When designing the bandwidth of ESO, the influence of total interference and sampling noise on the tracking performance of the system should be considered comprehensively.

3.4. **FOSMC design.** Substituting speed error e into (12), we obtain the derivative of ε

$$\dot{\varepsilon} = \frac{1}{2}\left[\ln\left(S(\varepsilon)+\underline{\eta}\right) - \ln\left(\bar{\eta} - S(\varepsilon)\right)\right]' = m\left(\dot{e} - n\right) \tag{20}$$

where $m = \frac{1}{2\mu}\frac{1}{\left[1/\left(S(\varepsilon)+\underline{\eta}\right)\right]-\left[1/\left(S(\varepsilon)-\bar{\eta}\right)\right]}$, $n = \frac{\dot{\mu}e}{\mu}$.

In order to obtain better tracking performance and reduce system chattering, a new fractional-order sliding mode surface is designed as

$$s = c\varepsilon + \sigma D^{\kappa-1}\left[\mathrm{sig}(\varepsilon)^{\gamma}\right] \tag{21}$$

where $\mathrm{sign}(\cdot)$ is the standard symbolic function, $\mathrm{sig}(\varepsilon)^{\gamma} = |\varepsilon|^{\gamma}\mathrm{sign}(\varepsilon)$, $c > 0$, $\sigma > 0$, $0 < \kappa < 1$, $0 < \gamma < 1$.

The derivative of (21) can be expressed as

$$\begin{aligned} \dot{s} &= c\dot{\varepsilon} + \sigma D^{\kappa}\left[\mathrm{sig}(\varepsilon)^{\gamma}\right] \\ &= cm\left(\dot{e} - n\right) + \sigma D^{\kappa}\left[\mathrm{sig}(\varepsilon)^{\gamma}\right] \\ &= cm\left(\alpha_v \dot{i}_q + F_v - \dot{v}^* - n\right) + \sigma D^{\kappa}\left[\mathrm{sig}(\varepsilon)^{\gamma}\right] \end{aligned} \tag{22}$$

To ensure the rapid convergence of the system state, the feedback control law is designed as

$$u_s = \frac{1}{\alpha_v}n - \frac{1}{cm\alpha_v}\left\{\sigma D^{\kappa}\left[\mathrm{sig}(\varepsilon)^{\gamma}\right] + k_1\mathrm{sign}(s) + k_2 s\right\} \tag{23}$$

Finally, the control law of speed loop can be designed as

$$i_q^* = \frac{1}{\alpha_v}\left(\dot{v}^* + n - \hat{F}_v\right) - \frac{1}{cm\alpha_v}\left\{\sigma D^{\kappa}\left[\mathrm{sig}(\varepsilon)^{\gamma}\right] + k_1\mathrm{sign}(s) + k_2 s\right\} \tag{24}$$

where k_1 and k_2 are positive constants, $k_1 > \left|cm\left(F_v - \hat{F}_v\right)\right| + k_3$, $k_3 > 0$.

3.5. **Stability analysis.** In order to check that the PMLSM drive system is stable under the action of the proposed controller, Lyapunov function can be constructed as

$$V = \frac{1}{2}s^2 \tag{25}$$

Taking the derivative of (25), yields

$$\begin{aligned} \dot{V} &= s\dot{s} \\ &= s\left\{cm\left(\alpha_v \dot{i}_q + F_v - \dot{v}^* - n\right) + \sigma D^{\kappa}\left[\mathrm{sig}(\varepsilon)^{\gamma}\right]\right\} \\ &= s\left[cm\left(F_v - \hat{F}_v\right) - k_1\mathrm{sign}(s) - k_2 s\right] \\ &= s\left[cm\tilde{F}_v - k_1\mathrm{sign}(s) - k_2 s\right] \end{aligned} \tag{26}$$

where $\tilde{F}_v = F_v - \hat{F}_v$, when $k_1 > \left|cm\tilde{F}_v\right| + k_3$, $\dot{V}$ can be expressed as

$$\begin{aligned} \dot{V} &\le \left(\left|cm\tilde{F}_v\right| - k_1\right)|s| - k_2 s^2 \\ &\le -k_3|s| - k_2 s^2 \\ &\le 0 \end{aligned} \tag{27}$$

According to the Lyapunov stability criterion, the proposed controller will make the whole system asymptotically stable and speed error eventually tends to zero.

4. Simulation and Experiment Validation.

4.1. Simulation validation. To verify the effectiveness of the designed controller, a simulation model of the PMLSM drive control system based on MATLAB/Simulink is built. In order to demonstrate the strong robustness of MFC to internal and external disturbances and the superiority of combining MFC with SMC, the proposed controller is compared to MFC [15] and PI in this article. ESO is used to estimate the unknown disturbance in MFC. On this basis, the speed tracking response and anti-interference performance of PMLSM at constant speed are analyzed under three control strategies when the motor encounters interference and motor parameters change. The block diagram of the PMLSM drive system control structure is illustrated in Figure 2. The main parameters of the PMLSM are given in Table 1. After a lot of repeated simulation and testing, we choose the following set of optimal parameters in the simulation. The parameters of PI in the speed loop are as follows: $k_{pv} = 5$, $k_{iv} = 80$. The parameters of the MFC controller in the speed loop are as follows: $\beta_1 = 2000$, $\beta_2 = 1000000$, $\alpha_v = 18$. The feedback controller is a proportional controller and its gain is 100. The parameters of the proposed controller in the speed loop are as follows: $\beta_1 = 2000$, $\beta_2 = 1000000$, $\alpha_v = 18$, $\sigma = 0.1$, $c = 10$, $\kappa = 0.5$, $\gamma = 0.5$, $k_1 = 1$, $k_2 = 800$. The PPF is selected as $\mu(t) = 0.395e^{-8t} + 0.005$, $\underline{\eta} = \bar{\eta} = 1$. The current loop parameters of the three controllers are $k_{pc} = 80$, $k_{ic} = 400$. The amplitude of i_q^* is limited to ± 2 A. The amplitude of u_d^* and u_q^* is limited to ± 120

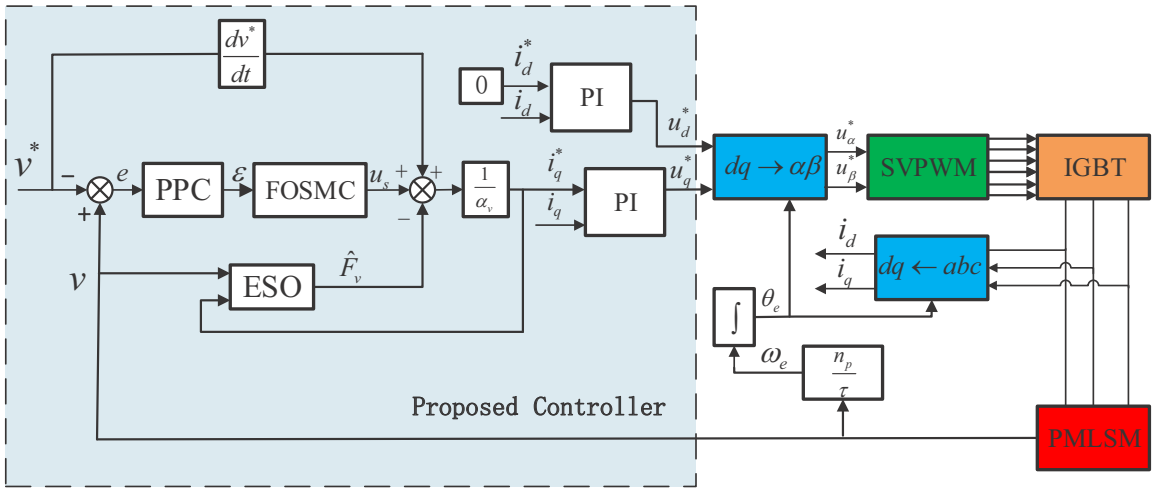

FIGURE 2. Block diagram of PMLSM drive system control structure

TABLE 1. Parameters of PMLSM

Description	Parameter	Value
Rated power	P_N	100 W
Rated voltage	U_N	220 V
Stator resistance	R_s	9.7 Ω
Stator inductance	L_d, L_q	43.3 mH
Mover mass	M	3.2 kg
Magnetic flux linkage	φ_f	0.165 Wb
Pole pairs	n_p	2
Pole pitch	τ	27 mm
Friction coefficient	B	0.2 N·s/m

V. The simulation sampling time is 10 μs. To evaluate the tracking performance of the proposed controller under different conditions, experiments are carried out under two conditions.

Case 1: The simulation time is set as 12 s and the expected speed of the PMLSM is 0.3 m/s. The initial external disturbance d is 0, which increases to 10 N when $t = 4$ s and decreases to -5 N when $t = 8$ s. The speed tracking response results of the three controllers are depicted in Figure 3(a). In the initial stage, a large overshoot occurs in PI and it takes the longest time to reach the given speed. MFC has no overshoot, but the rising speed is slower than the proposed method and the time to reach the given speed is longer than the proposed method. Since the proposed control method and MFC observe the total disturbance through ESO, the speed fluctuation range is smaller and the time required to reach the given speed is shorter when the disturbance is abrupt. At the same time, the feedback controller in the proposed controller is designed as FOSMC, which improves the speed tracking precision and reduces chattering. In addition, PI and MFC do not use PPF. When affected by external disturbances, PI and MFC will produce large tracking errors and exceed the prescribed limits. However, the speed tracking error using the proposed controller is small. The error is always within the prescribed range, although it is affected by external disturbance. The simulation results are depicted in Figure 3(b). In addition, it can be seen from Figure 3(c) that when the external disturbance changes, the electromagnetic thrust response time of the proposed method is the fastest and the most stable. ESO estimates of unknown disturbances to the system are depicted in Figure 3(d).

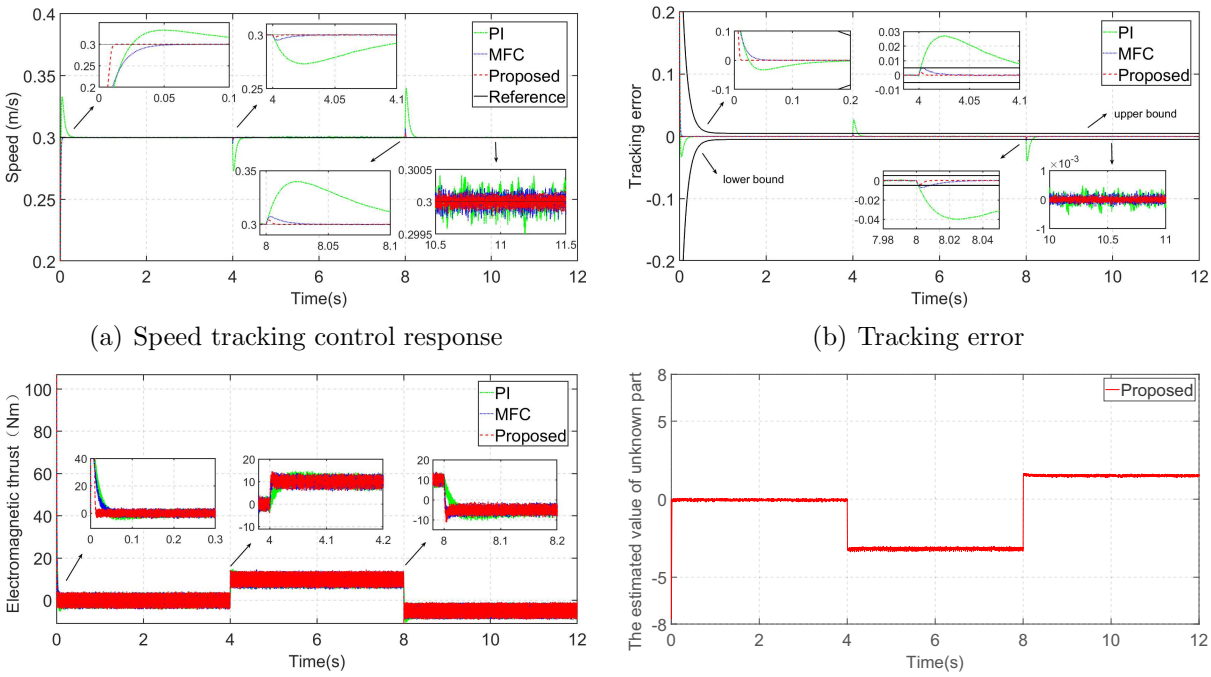

(a) Speed tracking control response

(b) Tracking error

(c) Electromagnetic thrust

(d) The estimated value of F_v

FIGURE 3. (color online) Simulation results in case 1

Case 2: In order to prove the robustness of the proposed method to the parameter perturbation of PMLSM, the motor parameters are changed under the same dynamic performance test conditions with case 1. The friction coefficient B and flux parameters φ_f are set to $2B$ and $1.5\varphi_f$ when respectively $t = 6$ s and compared with the parameter perturbation under PI and MFC. The simulation results are provided in Figure 4. As

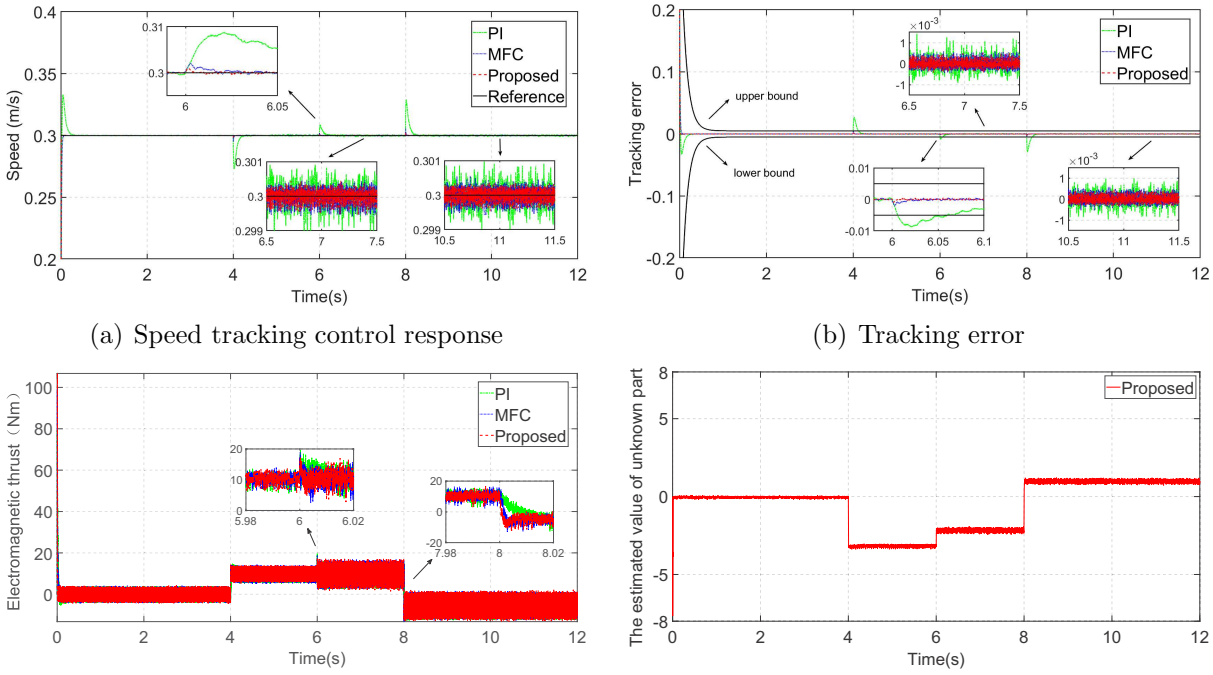

(a) Speed tracking control response

(b) Tracking error

(c) Electromagnetic thrust

(d) The estimated value of F_v

FIGURE 4. (color online) Simulation results in case 2

can be seen from Figure 4(a) and Figure 4(b), PI has a great imbalance when the motor parameters are perturbed. The speed fluctuation becomes significantly larger, while the speed fluctuation of MFC is smaller than PI. Since the proposed controller is based on the ULM and is not highly dependent on the parameters of PMLSM, the speed is least affected by the motor parameters change. When the disturbance and the motor parameters change, the proposed controller has the advantages of small overshoot, short response time, and high tracking precision. The electromagnetic thrust is depicted in Figure 4(c). It is obvious that the proposed method takes the shortest time to stabilize electromagnetic thrust and has the best effect on suppressing electromagnetic thrust pulsation. Unknown disturbances are estimated and feedforward compensated to the speed loop through ESO, as depicted in Figure 4(d).

4.2. **Experimental analysis.** To further prove the superiority of the proposed control method, a PMLSM driver platform based on dSPACE is built. It is composed of PMLSM, dSPACE DS1104 base board, incremental encoder, drive board, and host PC, as shown in Figure 5. The dSPACE DS1104 base board can be connected with Simulink in the host PC to realize the construction of a real-time control system. It also contains four 12-bit and one 16-bit analog to digital conversion (ADC) channels. The drive board contains a rectifier, inverter and two Hall current sensors. The three-phase voltage is converted into direct current voltage by the rectifier, which serves as the DC voltage of the inverter. The inverter is composed of three sets of IGBT with switching frequency of 5 Khz and dead time of 5 μs. The host PC controls the dSPACE output space vector pulse width modulation (SVPWM) signals to control the inverter, which can invert the DC voltage into AC voltage and supply power to the linear motor. The incremental encoder is used to receive the displacement signal of PMLSM and Hall sensors are used to collect the three-phase current signals. The software ControlDesk is used to control the running of PMLSM and make real-time data measurements. In addition, the speed loop sampling

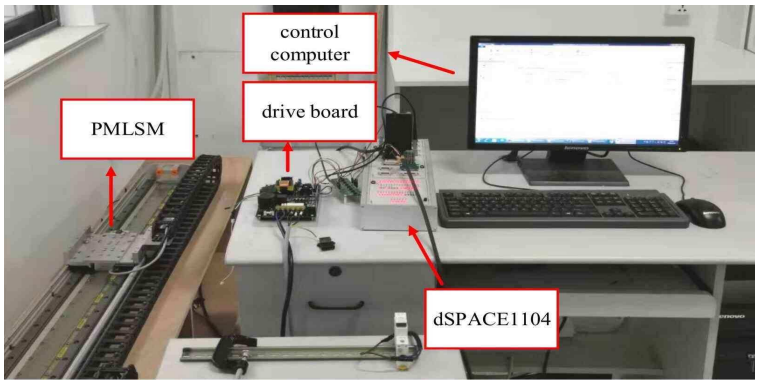

(a) Experimental platform setup

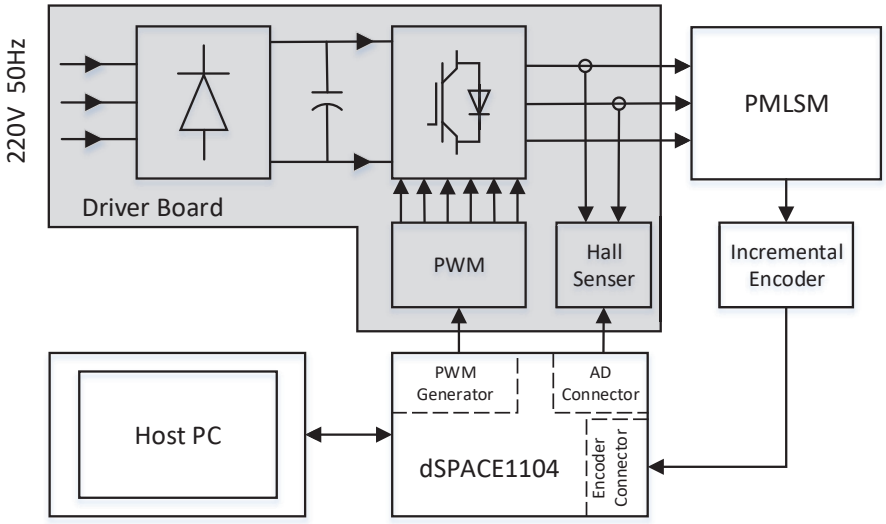

(b) Topology of experimental platform

FIGURE 5. Experimental system

frequency is set to 2500 Hz and the current loop sampling frequency is set to 5000 Hz of the system.

The parameters of PMLSM are the same with Table 1. A set of optimal parameters used in the experiment of each control strategy is finally determined as follows after a lot of repeated testing and verification. The parameters of PI in the speed loop are set to $k_{pv} = 30$, $k_{iv} = 800$. The parameters of MFC in the speed loop are set to $\beta_1 = 300$, $\beta_2 = 22500$, $\alpha_v = 18$. The feedback controller is a proportional controller and its gain is 300. The parameters of the proposed controller in the speed loop are set to $\beta_1 = 300$, $\beta_2 = 22500$, $\alpha_v = 18$, $\sigma = 0.1$, $c = 10$, $\kappa = 0.5$, $\gamma = 0.5$, $k_1 = 1$, $k_2 = 100$. The PPF is selected as $\mu(t) = 0.38e^{-8t} + 0.02$, $\underline{\eta} = \bar{\eta} = 1$. The current loop parameters of the three controllers are set to $k_{pc} = 80$, $k_{ic} = 400$. The amplitude of i_q^* is limited to ± 2.5 A. The amplitudes of u_d^* and u_q^* are limited to ± 120 V.

Case 1: The reference speed is set as a step signal of 0.2 m/s. The experimental results are provided in Figure 6. It can be seen from Figure 6(a) that the PI has the largest overshoot, while the proposed method has the smallest overshoot and the shortest rising time. In addition, the proposed control method uses PPC, which keeps the PMLSM speed tracking error within the prescribed range, as shown in Figure 6(b). Designing a feedback controller as FOSMC can make the speed error converge in a very short time and make

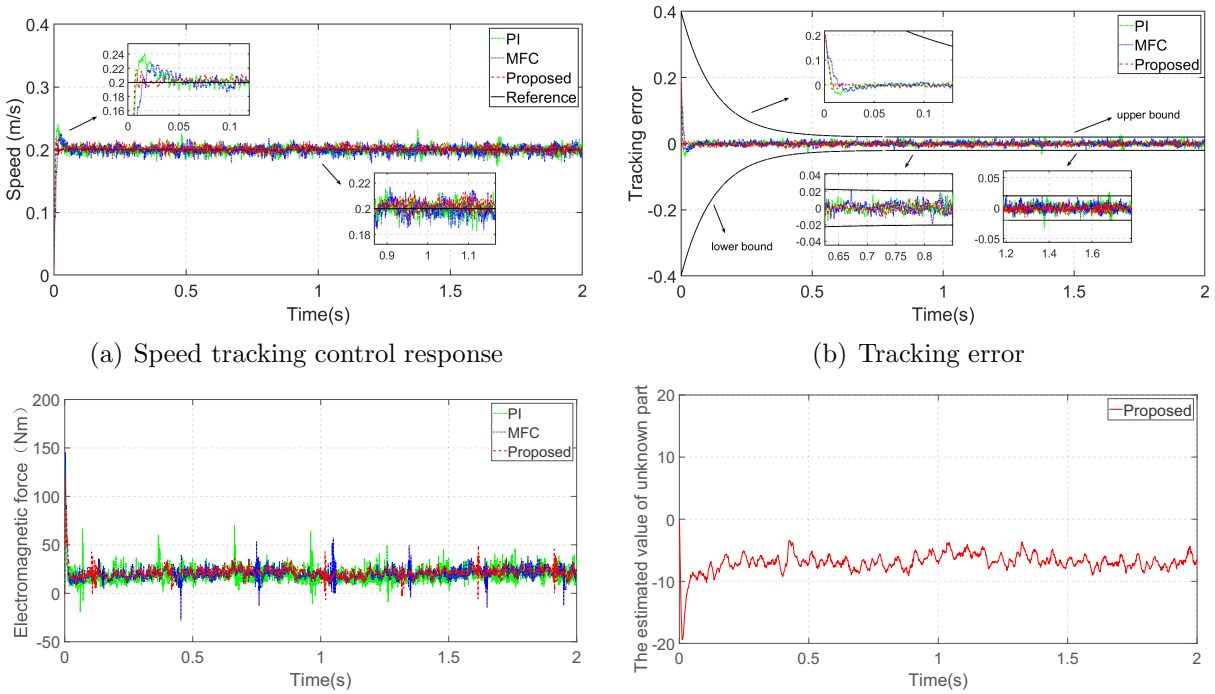

(a) Speed tracking control response

(b) Tracking error

(c) Electromagnetic thrust

(d) The estimated value of F_v

FIGURE 6. (color online) Experimental results in case 1

the speed of the motor have higher precision. PMLSM will meet uncertain disturbance when it runs, MFC and the proposed method using ESO to estimate the disturbance accurately and feed-forward compensation to the speed loop controller. Figure 6(d) shows the values of unknown disturbances estimated by ESO. Therefore, MFC and the proposed method have better steady-state performance than PI. In addition, the electromagnetic thrust fluctuation range of the proposed method is significantly smaller than PI and MFC, which is depicted in Figure 6(c).

Case 2: The reference speed step signal of 0.3 m/s is given to further validate the performance of PMLSM in the proposed method. The proposed method has the minimum overshoot, the fastest dynamic response speed, and the minimum steady-state error, as shown in Figure 7. The proposed method has good anti-interference and robustness, although the motor will be affected by the friction between the actuator and the track and has uncertain disturbance.

5. **Conclusions.** A prescribed performance based model-free fractional-order sliding mode control is proposed in this paper for precise speed tracking and robust control of PMLSM. The speed loop ULM is established based on the input and output of PMLSM and the unknown disturbances in the ULM are estimated by ESO. A new FOSMC is given as the feedback controller with the purpose of achieving fast convergence of system state variables. To limit the tracking error within the prescribed range, the PPC is adopted to limit the overshoot of motor speed and reduce the steady-state error to a certain extent. Simulation and experimental results prove that the proposed control algorithm can effectively reduce the influence of internal and external total disturbance and parameters change on the speed. In addition, the proposed control improves the dynamic response speed of PMLSM and strengthens the robustness of the system. In the future, we will try to improve the experimental device and verify the controller performance when PMLSM

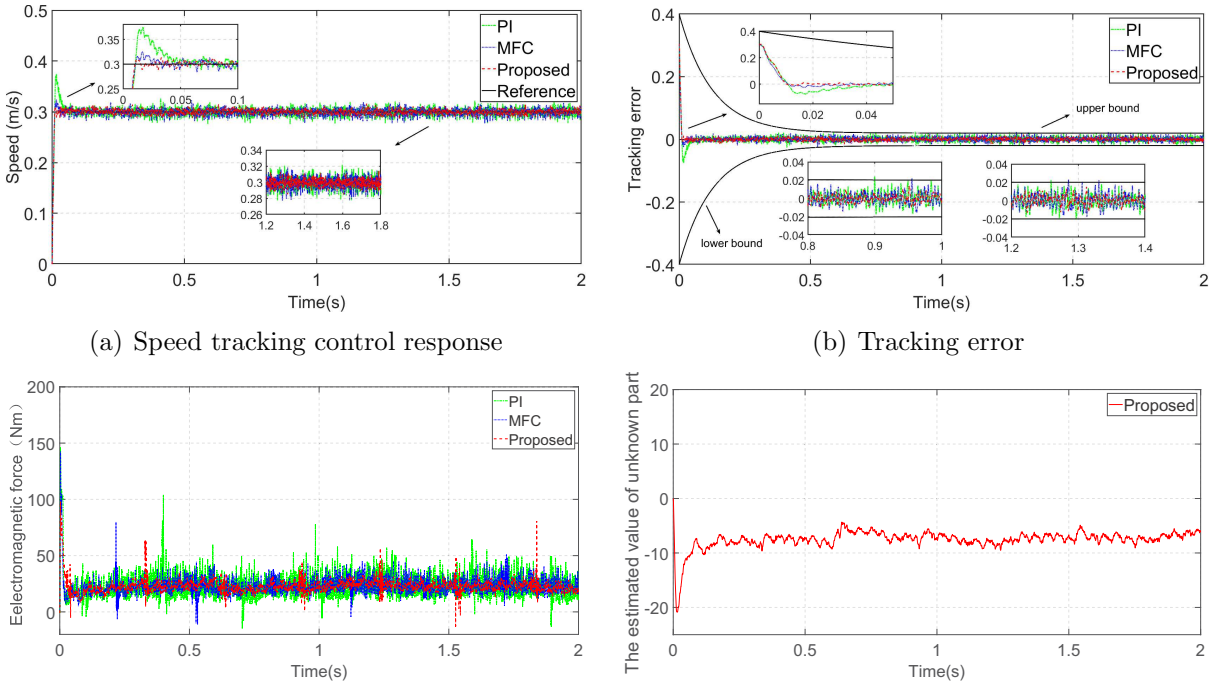

(a) Speed tracking control response

(b) Tracking error

(c) Electromagnetic thrust

(d) The estimated value of F_v

FIGURE 7. (color online) Experimental results in case 2

is running with load and parameter variations so that the experimental verification can be more complete.

Acknowledgment. This work is partially supported by the National Natural Science Foundation of China (Grant No. 62222307, No. 61973140) and the Natural Science Foundation of Jiangsu Province (Grant No. BK20211235); the authors also gratefully acknowledge the helpful comments and suggestions of the reviewers, which have improved the presentation.

REFERENCES

[1] F. F. M. E. Sousy and K. A. Abuhasel, Nonlinear robust optimal control via adaptive dynamic programming of permanent-magnet linear synchronous motor drive for uncertain two-axis motion control system, *IEEE Trans. Industry Applications*, vol.50, no.9, pp.1940-1952, 2020.

[2] D. Xu, W. Zhang, P. Shi and B. Jiang, Model-free cooperative adaptive sliding-mode-constrained-control for multiple linear induction traction systems, *IEEE Trans. Cybernetics*, vol.50, no.9, pp.4076-4086, 2020.

[3] K. Cho, J. Kim, S. B. Choi and O. Sehoon, A high-precision motion control based on a periodic adaptive disturbance observer in a PMLSM, *IEEE/ASME Trans. Mechatronics*, vol.20, no.5, pp.2158-2171, 2015.

[4] Q. Lu, B. Wu, Y. Yao, Y. Shen and Q. Jiang, Analytical model of permanent magnet linear synchronous machines considering end effect and slotting effect, *IEEE Trans. Energy Conversion*, vol.35, no.1, pp.139-148, 2020.

[5] D. Xu, B. Ding, B. Jiang, W. Yang and P. Shi, Nonsingular fast terminal sliding mode control for permanent magnet linear synchronous motor via high-order super-twisting observer, *IEEE/ASME Trans. Mechatronics*, vol.27, no.3, pp.1651-1659, 2022.

[6] R. Yang, M. Wang, L. Li, G. Wang and C. Zhong, Robust predictive current control of PMLSM with extended state modeling based Kalman filter: For time-varying disturbance rejection, *IEEE Trans. Power Electronics*, vol.35, no.2, pp.2208-2221, 2020.

[7] R. Yang, L. Li, M. Wang and C. Zhang, Force ripple compensation and robust predictive current control of PMLSM using augmented generalized proportional-integral observer, *IEEE Journal of Emerging and Selected Topics in Power Electronics*, vol.9, no.1, pp.302-315, 2021.
[8] S. Chen and T. Liu, Intelligent tracking control of a PMLSM using self-evolving probabilistic fuzzy neural network, *IET Electric Power Applications*, vol.11, no.6, pp.1043-1054, 2017.
[9] P. Wang, Y. Xu, R. Ding, W. Liu, S. Shu and X. Yang, Multi-kernel neural network sliding mode control for permanent magnet linear synchronous motors, *IEEE Access*, vol.9, pp.57385-57392, 2021.
[10] B. Ding, D. Xu, W. Yang, K. Bi and W. Yan, Nonsingular terminal sliding mode control for PMLSM based on disturbance observer, *2020 IEEE 9th Data Driven Control and Learning Systems Conference*, pp.850-854, 2020.
[11] D. Fu, X. Zhao and J. Zhu, A novel robust super-twisting nonsingular terminal sliding mode controller for permanent magnet linear synchronous motors, *IEEE Trans. Power Electronics*, vol.37, no.3, pp.2936-2945, 2022.
[12] H. Jin and X. Zhao, Approach angle-based saturation function of modified complementary sliding mode control for PMLSM, *IEEE Access*, vol.7, no.11, pp.126014-126024, 2019.
[13] X. Zhao and D. Fu, Adaptive neural network nonsingular fast terminal sliding mode control for permanent magnet linear synchronous motor, *IEEE Access*, vol.7, pp.180361-180372, 2019.
[14] K. Zhang, L. Wang and X. Fang, High-order fast nonsingular terminal sliding mode control of permanent magnet linear motor based on double disturbance observer, *IEEE Trans. Industry Applications*, vol.58, no.3, pp.3696-3705, 2022.
[15] M. Fliess and C. Join, Model-free control, *International Journal of Control*, vol.86, no.12, pp.2228-2252, 2013.
[16] T. Li and X. Liu, Model-free non-cascade integral sliding mode control of permanent magnet synchronous motor drive with a fast reaching law, *Symmetry*, vol.13, no.9, 1680, DOI: 10.3390/sym13091680, 2021.
[17] Y. Zhou, H. Li and H. Yao, Model-free control of surface mounted PMSM drive system, *2016 IEEE International Conference on Industrial Technology*, pp.175-180, 2016.
[18] Y. Zhang, J. Jin and L. Huang, Model-free predictive current control of PMSM drives based on extended state observer using ultralocal model, *IEEE Trans. Industrial Electronics*, vol.68, no.2, pp.993-1003, 2021.
[19] L. Yan, Y. Chen and H. Ahn, Fractional-order iterative learning control for fractional-order linear systems, *Asian Journal of Control*, vol.13, pp.54-63, 2011.
[20] M. Zhuang and Q. Zhu, The internal mode fractional-order PID control based on neural network for the temperature of air-conditioned rooms, *International Journal of Innovative Computing, Information and Control*, vol.17, no.3, pp.1019-1028, 2021.
[21] X. Lin, J. Liu, F. Liu, Z. Liu, Y. Gao and G. Sun, Fractional-order sliding mode approach of buck converters with mismatched disturbances, *IEEE Trans. Circuits and Systems I: Regular Papers*, vol.68, no.9, pp.3890-3900, 2021.
[22] Q. Teng, D. Xu and W. Yang, An adaptive fractional-order sliding mode control for virtual synchronous generator in microgrid, *ICIC Express Letters*, vol.16, no.9, pp.983-991, 2022.
[23] S. Chen, H. Chiang, T. Liu and C. Chang, Precision motion control of permanent magnet linear synchronous motors using adaptive fuzzy fractional-order sliding-mode control, *IEEE/ASME Trans. Mechatronics*, vol.24, no.2, pp.741-752, 2019.
[24] Z. Kuang, H. Gao and M. Tomizuka, Precise linear-motor synchronization control via cross-coupled second-order discrete-time fractional-order sliding mode, *IEEE/ASME Trans. Mechatronics*, vol.26, no.1, pp.358-368, 2021.
[25] R. Mei and R. Li, Fault-tolerant tracking control for unmanned helicopter altitude and attitude system based on prescribed performance method, *International Journal of Innovative Computing, Information and Control*, vol.15, no.6, pp.2247-2258, 2019.
[26] M. Ma, K. Zhao and S. Song, Adaptive sliding mode guidance law with prescribed performance for intercepting maneuvering target, *International Journal of Innovative Computing, Information and Control*, vol.16, no.2, pp.631-648, 2020.
[27] Q. Liu, D. Xu, B. Jiang and Y. Ren, Prescribed-performance-based adaptive control for hybrid energy storage systems of battery and supercapacitor in electric vehicles, *International Journal of Innovative Computing, Information and Control*, vol.16, no.2, pp.571-583, 2020.
[28] S. Dai, S. He, X. Chen and X. Jin, Adaptive leader-follower formation control of nonholonomic mobile robots with prescribed transient and steady-state performance, *IEEE Trans. Industrial Informatics*, vol.16, no.6, pp.3662-3671, 2020.

[29] Y. Wang, H. Wang and M. Fu, Prescribed performance trajectory tracking control of dynamic positioning ship under input saturation, *Transactions of the Institute of Measurement and Control*, vol.44, no.1, pp.30-39, 2022.

[30] Y. Sun and Y. Liu, Adaptive synchronization of fractional-order chaotic neural networks with unknown parameters and time-varying delays, *International Journal of Innovative Computing, Information and Control*, vol.16, no.2, pp.649-661, 2020.

Author Biography

Jing Hu received the B.S. degree in electrical engineering and automation from Jiangnan University, Wuxi, China, in 2018. He is currently pursuing the M.S. degree in electrical engineering with Jiangnan University, Wuxi, China. His current research interests include sliding mode control and motor control.

Dezhi Xu received the Ph.D. degree in control theory and control engineering from Nanjing University of Aeronautics and Astronautics, China, in 2013.

He was a Visiting Fellow with the Department of Biomedical Engineering, City University of Hong Kong, China, from 2018 to 2019. He is currently a Professor and Doctoral Supervisor with the Jiangnan University. His research interests include data-driven control, fault diagnosis and fault-tolerant control, multi-agent systems and cyber-physical systems, technologies of renewable energy, motor control, and smart grid.

Dr. Xu was supported by the National Natural Science Fund for Excellent Young Scientists Fund Program in 2022. He was a recipient of the First Class Prize of Science and Technology Progression from the China General Chamber of Commerce in 2016, and the Best Young Scholar of Jiangnan University in 2022. He was a Guest Editor for the International Journal of Innovative Computing, Information and Control and the Electric Power. He currently serves as an Editorial Board Member for the International Journal of Innovative Computing, Information and Control, the Electric Power, the Electrotechnical Application and the Electrical Engineering. He is a Committee Member of the Association of Energy Internet, and Trusted Control in Chinese Association of Automation (CAA), and the Energy Storage in China Renewable Energy Society (CRES).

Weiming Zhang received his M.S. degree in control engineering from Jiangnan University, Wuxi, China in 2020. He is currently working toward the Ph.D. degree in control engineering with Jiangnan University, Wuxi, China. His current research interests include data-driven control, model-free adaptive control and multiagent systems.

Weilin Yang received his B.Eng. degree in machine design & manufacture and their automation from University of Science and Technology of China, Hefei, China, in 2009, and the Ph.D. degree in mechanical engineering from City University of Hong Kong, Hong Kong, in 2013.

Dr. Yang was a postdoctoral researcher at Masdar Institute of Science and Technology (now Khalifa University), Abu Dhabi, UAE, 2013-2016. He was a research engineer of General Electric (GE) Global Research, Shanghai, 2016-2017. He joined Jiangnan University in July 2017, where he is currently an Associate Professor. His research interests include modeling and control of energy systems, robust model predictive control, and dada-driven control.